Under-measured Precipitation Extremes from Manual Gauge Observations over the Northern Regions

Xicai Pan[1], Daqing Yang[2], Kwok Pan Chun[3], Jiabao Zhang[1*], Yanhui You[4]

[1]State Key Laboratory of Soil and Sustainable Agriculture, Institute of Soil Science, Chinese Academy of Sciences, 71 East Beijing Road, 210008, Nanjing, China

[2] National Hydrology Research Centre, Environment Canada, 11 Innovation Boulevard, Saskatoon, Canada

[3]Department of Geography, Hong Kong Baptist University, Hong Kong SAR, China

[4]State Key Laboratory of Frozen Soil Engineering, Northwest Institute of Eco-Environment and Resources, Chinese Academy of Sciences, 320 Donggang West Road, 730000, Lanzhou, China

*E-mail: email: jbzhang@issas.ac.cn

Keywords: precipitation extremes, manual gauge observation, bias correction, under-measured, meteorological disasters

Abstract

Extreme precipitation is a major issue for regional climate, hydrology, and safety of society. Our knowledge of extreme precipitation is poor because of difficulties in gauge observations and biases in regional and global datasets, in particular over the snow dominated regions. Here we investigate and report the distribution and magnitude of under-measured of precipitation extremes due to biases in manual gauge observations in the high latitudes (over 45ºN), using historical data during 1973-2004. We find remarkable patterns in under-measured of the long-term mean daily maximum precipitation and their association to regional climatic regimes. In contrast to relatively small under-measured (less than 5 mm) of rainfall extremes, the biases in snowfall extremes are very serious, with the regional high values over 15 mm along the Ural Mountains and the coasts of east Asia, Greenland, in particular northern Eurasia coasts. The frequency distribution of observed daily snow extremes underestimate significantly the higher risk events over the high latitudes. These results clearly demonstrate the urgent need to review and update precipitation datasets including recent automatic gauge observations and the knowledge of climate regimes and extremes over the broader northern regions.

1. Introduction

Extreme precipitation is a major concern for regional climate, hydrology, and safety of society, because heavy precipitation events trigger serious hazards, such as floods, landslides, and soil erosion in warm regions/seasons (O'Gorman, 2015), and snow-related disasters in the cold regions/seasons, including avalanche, building collapse due to heavy snow load, shutdowns of highway traffic and runway operations (López-Moreno and Vicente-Serrano, 2011). Our knowledge of extreme precipitation is poor because of difficulties in precipitation observations by gauges, particularly for snowfall in the northern regions (Goodison et al., 1998; Yang et al., 2005; Sugiura et al., 2006). Due to wind-induced gauge under-catch, wetting and evaporation losses, and trace amount of precipitation (Goodison et al., 1998; Yang et al., 1998a; Legates and Willmott, 1990; Fuchs et al., 2001), the biases (under-measured) in gauge measurements are very large, up to 50-100%, for snowfall over the cold regions (Yang et al., 2005). Most regional/global precipitation datasets have large uncertainties for the northern regions due to sparse observation networks, space-time discontinuities of precipitation data and biases in gauge observations (Behrangi et al., 2018; Walsh et al., 1998; Yang et al., 1999a). Investigations based on these datasets may lead to incorrect results in regional precipitation climate, including the characteristics of extreme events (Prein and Gobiet, 2016; Behrangi et al., 2016, 2018).

Corrections of the known biases are necessary to develop reliable precipitation dataset for regional hydrology and climate investigations, including trend analyses. In order to quantify the systematic errors in precipitation measurements, intercomparison experiments have been carried out for the national standard gauges, such as the World Meteorological Organization (WMO) Solid Precipitation Measurement Intercomparison study during 1986 to 1992 (Goodison et al., 1988, 1998). The WMO project developed bias-correction methods for many national gauges (Goodison et al., 1998; Yang et al., 1995,1998a, 1999a,

c), quantified wind shield effects on national gauge performance (Yang et al., 1999b), and documented incompatibility in national gauge observations (Yang et al., 2001). Applications of the WMO results have produced reliable precipitation data over many countries and large regions (Melcalfe et al., 1993; Yang, 1999; Yang et al., 1998b, 1999b, 2005; Yang and Ohata, 2001; Zhang et al., 2004; Ye et al., 2004; Adam and Lettenmaier, 2003), and these datasets have significantly improved our understanding of cold region climate and hydrology, including regional climate regime and change (Ding et al., 2007; Li et al., 2018), basin water balance (Ye et al., 2012), large-scale land surface modelling of the arctic hydrology system (Tian et al., 2007), and precipitation distribution and gradient across the Alaska-Yukon border (Scaff et al., 2015).

Because of the importance of heavy precipitation, particularly extreme snowfall hydrology and climate change analysis over the high latitudes, we generate a new daily maximum precipitation dataset from Yang et al. (2005). This dataset consists of daily precipitation time series for rain, snow and mixed phase at 1249 stations located above 45ºN during 1973-2004. We choose this time period when the manual gauges were the standard instruments for precipitation measurements over most northern countries. This long period is sufficient to examine precipitation characteristics, including the extremes, while avoiding the complication due to significant inconsistency between manual and automatic gauge measurements in recent years (Brandsma, 2014; Talchabhadel et al., 2017). It is important to point out that the bias corrections are conservative, because a threshold wind speed was set at 7 m s^{-1}, so as to avoid possible over corrections for higher wind conditions when blowing snow may occur and impact the reliability of the corrections methods (Yang et al., 2005). With the new dataset and statistical analysis, we quantify the magnitude of under-measured of daily maximum precipitation, namely bias-corrected precipitation minus observed ones, across the northern regions, and identify the potential impacts and consequences in large-scale climate and hydrology analyses and applications, including risk assessment and engineering designs.

2. Data and methods

The historical meteorological data used in this study were originated from the official archived dataset, Global Historical Climatology Network (GHCN, https://www.ncdc.noaa.gov/data-access/land-based-station-data/land-based-datasets/global-historical-climatology-network-ghcn). The historical precipitation observations were retrieved manually from the standard instruments of various gauges in different countries. Due to dominant solid precipitation across the northern regions, serious under-measured exists. Based on these data, Yang et al. (2005) conducted bias correction analysis and built a dataset of a total number of 4802 stations located above 45ºN during 1973-2004. The bias-correction methods used by Yang et al. (2005) are briefly summarized below. To account for trace events, wetting loss, evaporation loss, and wind-induced error in various gauges, a general statistically-based model is applied

$$P_c = P_m/\mathrm{CR}, \quad (1)$$

where P_c is the corrected precipitation, P_m is the measured precipitation, and CR is the catch ratio (%). CR is defined as a function of wind speed and air temperature (Goodison et al., 1998), and the function varies in different countries due to different gauge types and regional climate. Since the observations were retrieved manually from the standard instruments of manual gauges with a daily or sub-daily interval, the daily precipitation phases are determined by daily mean near-surface air temperature as rain: T_a >= 2 °C, mixed: -2 °C < T_a < 2 °C, and snow: T_a <= -2 °C (Yang et al., 1998a; Rajagopal and Harpold, 2016). It is important to note that this study uses a constant temperature threshold to determine precipitation phases without considering its spatial variation (Jennings et al., 2018).

To analyze the underestimation of precipitation extremes, a new dataset for daily maximum precipitation is derived from the original dataset based on a quality control as follows. This dataset consists of the highest daily precipitation time series for rain, snow and mixed phase at 1249 stations with over 15-year records for

the period of 1973-2004. The properties of the valid data at these stations are presented in Fig. 1. The indexes of yearly extreme precipitations used in this study include gauge measured daily maximum precipitation, Pm_{max}, bias-corrected daily maximum precipitation, Pc_{max}, and corresponding daily maxima for three phases, $Pm_{i,max}$, $Pc_{i,max}$, where i = {r, m, s} represent rain, mixed and snow. Instead of simply using less than 10% of missing data as selection criteria (e.g., Kunkel et al., 2007; Changnon, 2018), a more rigorous threshold is applied in this study. We reject a year if the fraction of missing data exceeded 5%, so as to ensure that annual maxima are extracted with a confidence of 95% for each station in the region.

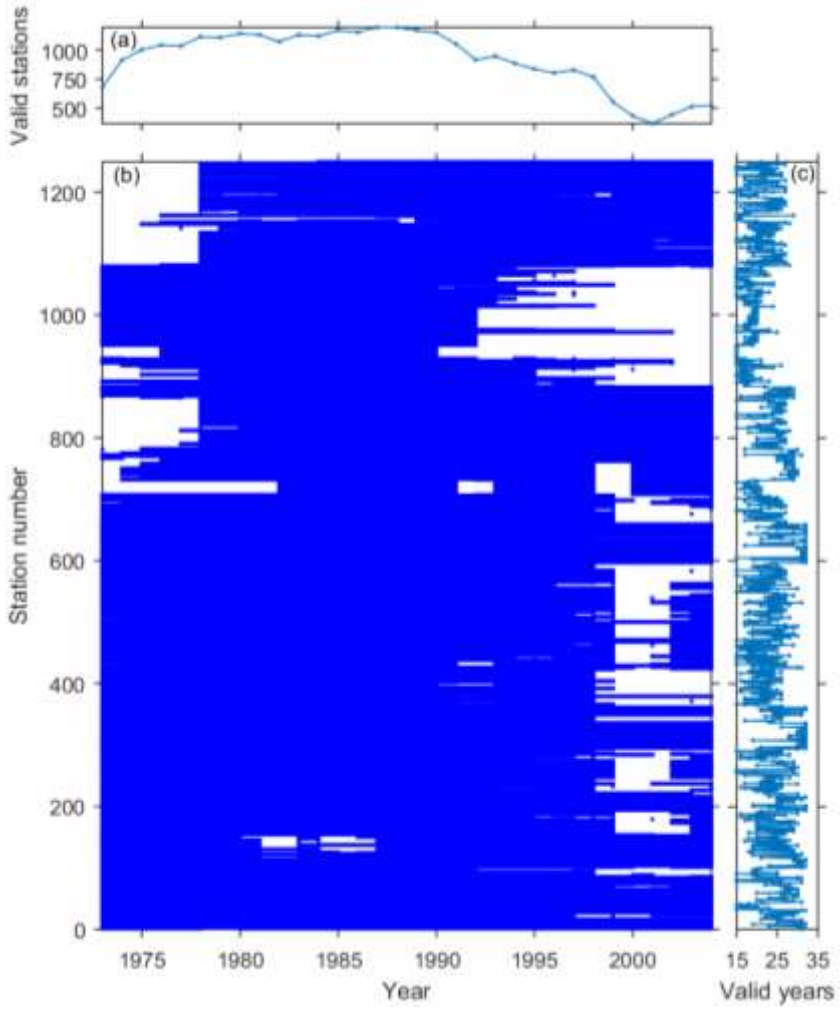

Figure 1. Properties of the selected station data. (a) A number of 1249 valid stations during the period from 1974 to 2004. (b) Data coverage over time for all stations. (c) Distribution of the numbers of valid years at the stations.

For fitting the distribution of the annual precipitation maxima, we use a three-parameter Generalized Extreme parametric framework (von Mises, 1954; Jenkinson, 1955), which is widely used for precipitation extreme distribution (Hanson and Vogel, 2008; Wilson and Toumi, 2005). Based on the extreme value theory, the generalized extreme value (GEV) distribution is used for estimating the frequency of the extremes occurring with a certain return level. The GEV distribution is parameterized with the location parameter μ, scale parameter σ and shape parameter ξ. The cumulative distribution function of the GEV distribution is

$$F(x;\mu,\sigma,\xi) = \exp\left(-\left(1+\xi\left(\frac{x-\mu}{\sigma}\right)\right)^{-\frac{1}{\xi}}\right), \quad (2)$$

and its probability distribution function is

$$f(x) = \begin{cases} \frac{1}{\sigma}\exp\left(-\left(1+\xi\left(\frac{x-\mu}{\sigma}\right)\right)^{-\frac{1}{\xi}}\right)\left(1+\xi\left(\frac{x-\mu}{\sigma}\right)\right)^{-1-1/\xi}, & \xi \neq 0 \\ \frac{1}{\sigma}\exp\left(-\frac{x-\mu}{\sigma}-\exp(-\frac{x-\mu}{\sigma})\right), & \xi = 0 \end{cases} \quad (3)$$

where the domain of σ and $1+\xi(x-\mu)/\sigma$ must be greater than zero, and μ and ξ can be any real value. In this study, the location, shape and scale parameters of the GEV distribution are estimated based on the maximum likelihood estimator (MLE) (Coles, 2001). The advantage of using MLE are that the estimated parameters are unbiased, and the standard errors of estimated parameters can be computed so as to derive confidence intervals of the estimate parameters. We use the confidence intervals of the estimated parameters to estimate the p-value of whether our correction can lead to significant different distribution parameters (i.e. location, scale and shape parameters).

3. Results

3.1. Under-measured of extreme precipitation

Daily precipitation maximum (P_{max}) at a given site may occur as rainfall, snowfall and mixed phase over large regions of various climate regimes. It is useful and important to identify the under-measured of the daily precipitation maxima for each phase. We used daily mean temperature to determine precipitation phases (Yang et al., 1998b; Rajagopal and Harpold, 2016), and produced mean P_{max} maps for rainfall, snowfall and mixed precipitation for the period 1973-2004 (Fig. 2).

For rainfall, we see high mean P_{max} values over 40 mm mainly in the mid latitude belt between 45ºN and 60ºN, and two regional peaks over 60 mm in northeastern Asia and eastern Europe along the 30th meridian east (Fig. 2a). The former is associated with the well-known East Asia monsoon (Ding and Chan, 2005), and the latter is mostly related with the Carpathians climate. While in the western hemisphere, the highest P_{max} along the East Coast gradually decrease westward, and abruptly increase in the west coast mountains due to orographic precipitation (Fig. 2a). This pattern is consistent with the general Canadian precipitation distribution (Shabbar et al., 1997). In addition, we also see low P_{max} values (less than 20 mm) in the coastal Polar Regions. Generally, as expected, most under-measured is less than 5 mm for rain (Fig. 2b) and the relative changes after the bias-corrections (Fig. 2c) are below 10%. Significant changes (5 – 10 mm), mainly associated with moderate and high P_{max}, occur near the east Asia coasts and Eastern Europe.

For snowfall, the mean P_{max} magnitude is much smaller than that for rain, and its distribution is also different. In the eastern hemisphere, the high values over 20 mm are mainly located along the Urals mountain and near the east Asia coasts. The former is dominated by orographic precipitation, and the latter is mainly controlled by coastal precipitation. We see serious under-measured (over 10 mm) in the islands and Peninsula, i.e. the Sakhalin and Kamchatka in east Asia, Eastern Europe and the coasts and islands around Kara Sea (Fig. 2e), with the relative change over 30% (Fig. 2f). In the western hemisphere, the high values above 20 mm mainly concentrate in eastern Canada and this pattern is consistent with the gauge observations.

For mixed precipitation, the magnitude of mean P_{max} is close to that for snowfall, with a similar distribution to rainfall P_{max}. However, a slightly shift of the high P_{max} zone (over 20 mm) occurs in between the western Europe along the 30th meridian east with high rainfall and the Ural mountains along the 60th meridian east with high snowfall. We found the bias-corrections significantly changed the P_{max} amounts by 10-15 mm over the coasts of Okhotsk and Bering seas, with the relative increase of 40% or more (Fig. 2i), although P_{max} pattern did not change much.

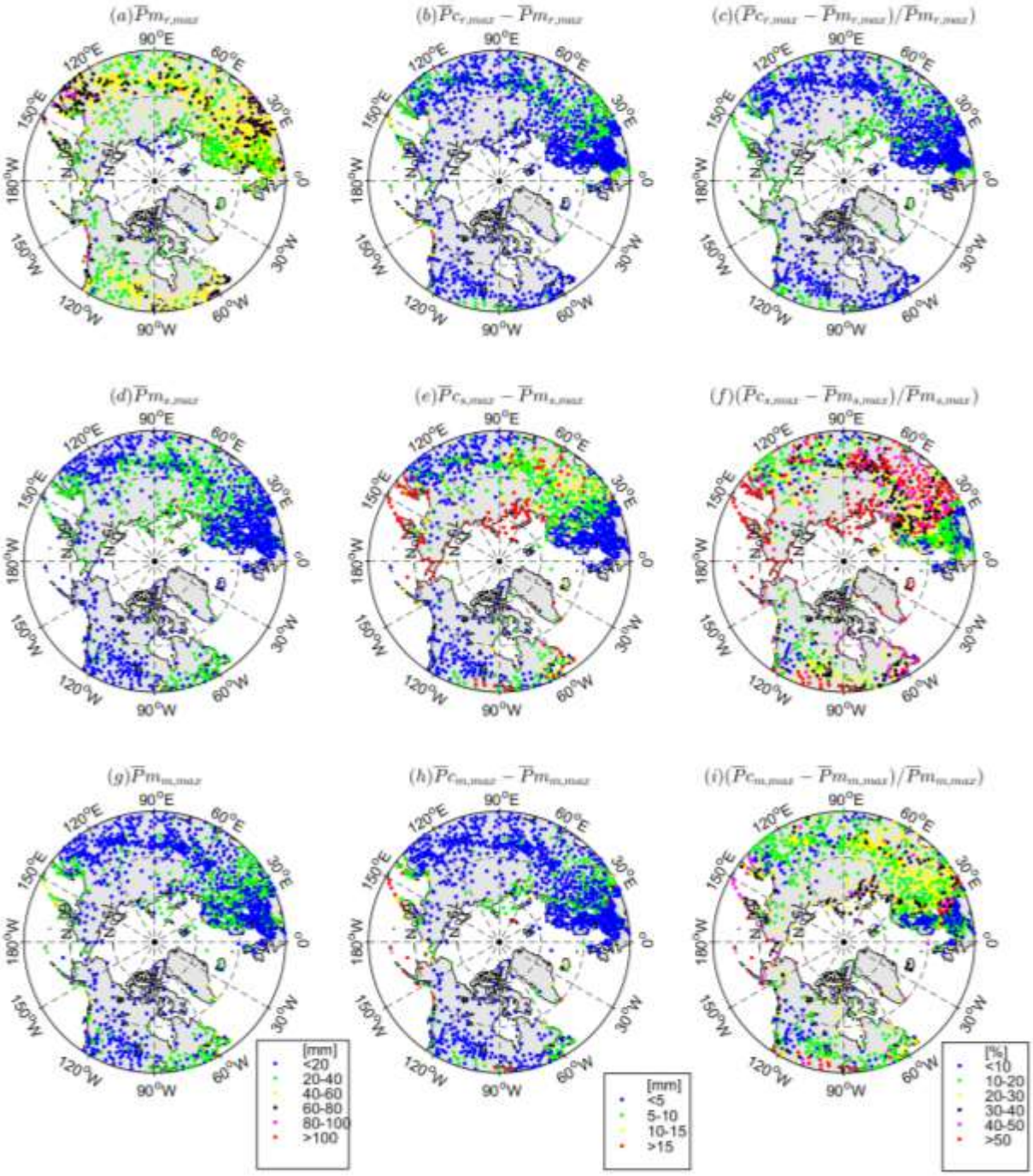

Figure 2. Under-measured patterns of extreme precipitation amount for three phases (rain, snow and mixed) in the northern regions. (a)-(c) show rather uniform distributions of absolute and relative changes in daily maximums for observed rain ($\overline{P}m_{\mathrm{r.max}}$) in comparison to the bias-corrected ones ($\overline{P}c_{\mathrm{r.max}}$). (d)-(f) show contrasting regional changes in daily maximum snowfall ($\overline{P}m_{\mathrm{s.max}}$). (g)-(i) show similar pattern as snow precipitation but relatively weaker for mixed precipitation.

3.2. Regional under-measured over the high latitudes

We found serious under-measured of snowfall extremes in the high latitude regions (over N60° latitude). Since undercatch of snowfall differs by gauge types, we examined the biases of P_{max} for four major regions/gauges within the polar regions, i.e. northern Russia (NRS), Alaska - United States (A-US), northern Canada (NCA) and Greenland (GL) (Fig. 3).

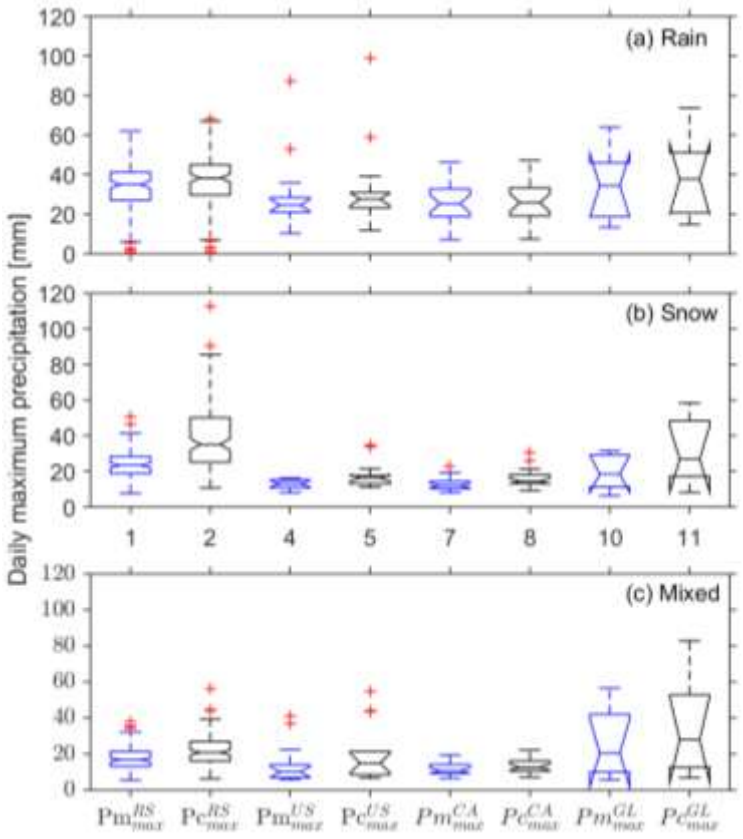

Figure 3. Regional under-measured of daily maximum precipitation in the polar regions (over N60° latitude). The black boxplots represent measured daily maximum precipitation in the regions of Russia, United States, Canada and Greenland (Pm_{max}^{RS}, Pm_{max}^{US}, Pm_{max}^{CA}, Pm_{max}^{GL}) and the blue boxplots represent the corrected ones Pc_{max}^{RS}, Pc_{max}^{US}, Pc_{max}^{CA}, Pc_{max}^{GL}). There are 136, 14, 24 and 7 stations in each region, respectively.

The median values of the observed mean rainfall P_{max} are about 25 mm for A-US and NCA, and 35 mm for GL and NRS, respectively. The biases (Fig. 3a) are less than 4 mm for all the regions. In contrast, the

median values of snowfall extremes range from 12 mm in NCA to 23 mm in NRS, and the average biases vary from 2 mm to 12 mm (Fig. 3b). We see most serious under-measured in NRS, about 12 mm (or 50%), on average, and even higher than 15 mm at some sites surrounding the coasts of the Kara Sea. This is mainly associated with high wind speeds and the heavy coastal precipitation across the Arctic Ocean and northern Eurasia. Whereas, the mean P_{max} in the regions of A-US and NCA are about half of NRS, since the precipitation climatology in northern North America is mainly characterized by light continental precipitation far from North Atlantic and North Pacific moisture sources (Gimeno et al., 2010). The under-measured is about 3 mm (or 23%) for both regions. The catch efficiency of the Canadian Nipher gauge is higher than the US 8-inch gauge (Yang et al., 2001; Goodiosn et al., 1998). The similar amount of corrections in A-US and NCA is due to lower wind speeds (mean about 2 m/s) at the A-US sites vs. high wind speed (mean of 4 m s^{-1}) in NCA (Fig. 4b). In GL, the observed snow P_{max} ranges from 6 mm to 32 mm, due to ample moisture transported from the Atlantic Ocean, with the mean bias up to 8 mm (or 45%).

For mixed P_{max}, the median values of the observed mean values are about 17 mm with an underestimate of about 4 mm (or 24%) in NRS (Fig. 3c). In the northern North America, both A-US and NCA have smallest mean extremes of 10 mm, but their correction amounts are 5 mm (48%) and 2 mm (18%), respectively. GL has the highest extremes (about 21 mm) with the most serious under-measured of 7 mm (36%) for 7 sites around Greenland, due to poor catch of the Hellman gauges and windy costal climate. Overall, the mixed extremes are much smaller than those for rainfall, although their biases are higher due to large undercatch of gauges for mixed precipitation.

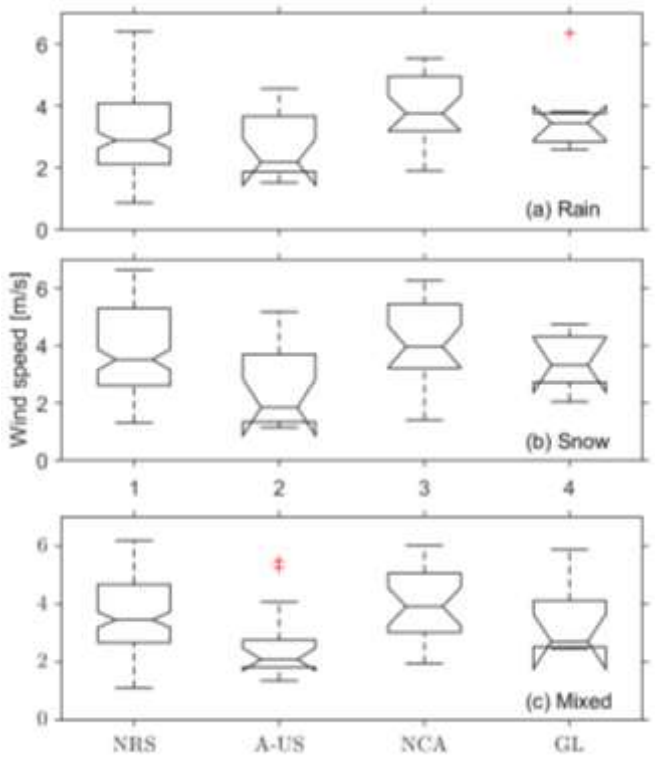

192 Figure 4 Corresponding mean wind speed for days with maximum precipitation during 1973-2004 for the
193 four regions in Fig. 3. Note that the high wind speeds over 7 m s^{-1} were replaced by a constant wind speed
194 of 7 m s^{-1} to avoid possible over bias-correction.

195 Through analyzing the under-measured of extreme precipitation amount, we identify the regions
196 susceptible to serious biases. Generally, under-measured of rainfall extremes in the middle latitudes is
197 relatively small (mostly less than 5 mm), and two regional high corrections (over 5 mm) are located in
198 northeastern Asia and eastern Europe along the 30th meridian east. In contrast, serious under-measured
199 mainly occurs for snowfall extremes, with regional highs (over 15 mm) along the Ural Mountains and the
200 coasts including east Asia, Greenland and northern Eurasia. These results demonstrate the serious under-
201 measured in extreme precipitation over the broader northern regions.

202 **3.3. Influence on frequency distribution**

203 In addition to regional hydrology and climate (Tian et al., 2007; Li et al., 2018), the under-measured can also

seriously distort the precipitation frequency distribution, thus influencing disaster warning and prevention. Bias corrections enhance value and range of the P_{max} time series non-uniformly at all stations in the study domain. To quantify the impact of bias corrections on P_{max} distribution, we examine changes in P_{max} frequency using the generalized extreme value (GEV) distribution model (Eq. 3). This model has three parameters, i.e. location (μ), scale (σ) and shape (ξ). The location (μ) parameter stands for the peak of probability distribution, and its change represents the overall shift of P_{max} series. The scale parameter is the scaled variance and the shape parameter governs the tail behavior of the distribution. The scale and shape parameters control the spread of extreme events. Particularly, change in the scale parameter affects extreme events distinctly for low and high return periods.

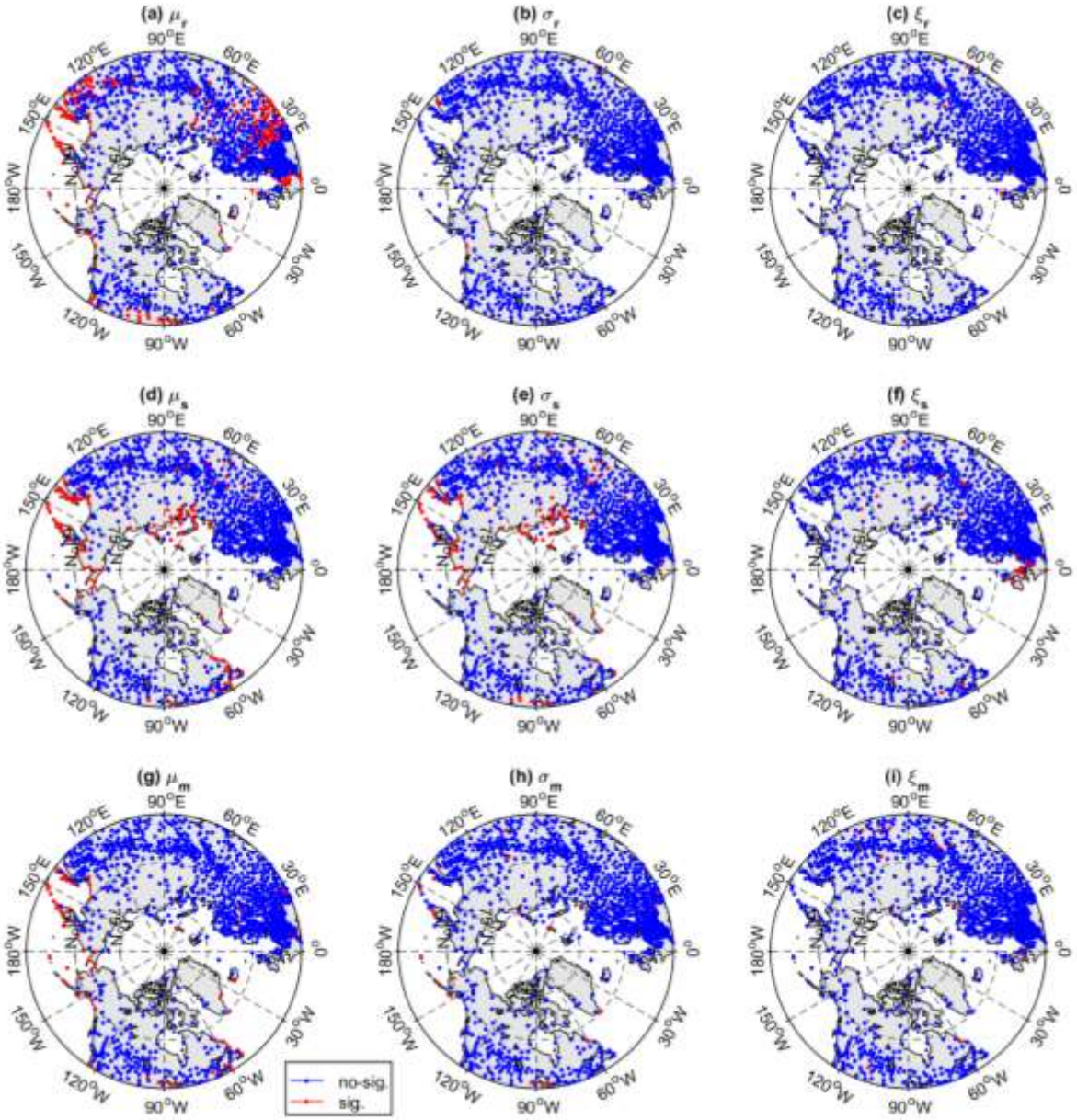

Figure 5 Impact of bias-corrections on the parameters of GEV distribution for rain (a, b, c), snow (d, e, f) and mixed (g, h, i) extremes. Red dots show stations with significant changes in GEV parameters at threshold level $\alpha = 0.05$; blue dots indicate insignificant ones.

Figure 5 shows different impacts of bias-correction on the GEV parameters by precipitation phases at all stations. For rainfall extremes, about 200 sites (or 16% out of 1249 sites) show significant shift in the location parameter, coincident with the sites with moderate and high mean P_{max} (Fig. 2a). As an example, Sodankyla in Finland (USAF ID: 028360) has an increase in the mean value by about 2 mm for rainfall; this is forest

with very low winds (Fig. 6a). For snowfall, both the mean peak and spread changed significantly at many sites (6% of stations). For example, Anadyr in Russia (USAF ID: 255630) in Fig. 6b shows a distinct transition from a heavy-tailed Fréchet distribution to a short-tailed negative-Weibull distribution. The P_{max} value for a 100-year return period changed from 55 mm d^{-1} to 101 mm d^{-1}. For mixed precipitation, the changes are similar to rainfall but only over 57 sites. Generally, bias corrections have less effect on the P_{max} frequency distribution for rain and mixed phase, while the changes in snow extremes are very significant and need proper attention in frequency analysis and related applications, such as snow load and other engineering designs. More work is necessary to determine the impact of P_{max} corrections to regional hydrology and engineering design and other applications.

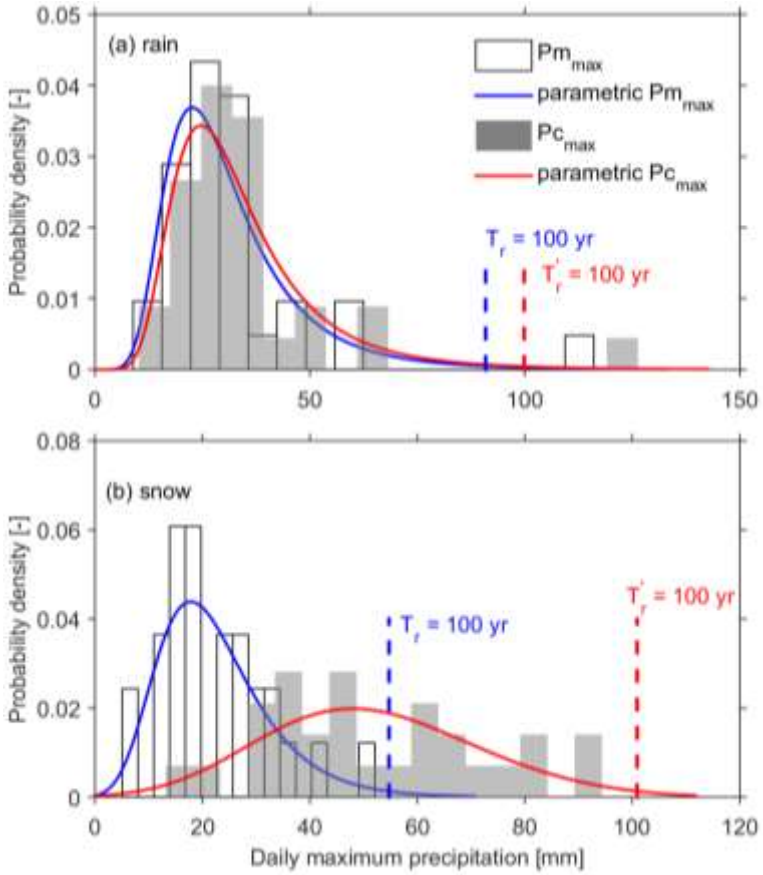

Figure 6. Frequency distributions of observed (Pm_{max}) and corrected (Pc_{max}) daily maximum precipitation. The blue and red curves represent the parametric GEV distribution. (a) A typical rain dominated station

(Sodankyla, Finland) with less change; (b) A typical snow dominated station (Anadyr, Russia) with big change in the P_{max} series for snow data. T_r and T_r' represent the 100-year return periods for the observed and corrected distributions, respectively.

4. Discussion and conclusions

This study investigates under-measured of precipitation extremes due to biases in gauge observations in the high latitudes (over 45ºN), using historical manual observations during 1973-2004. We find remarkable patterns in under-measured of the long-term mean daily maximum precipitation and their association to regional climatic regimes. In general, the P_{max} distributions for the three phases are consistent with our previous understanding of regional precipitation patterns derived from the gauge-measured data (e.g., Hartmann, 2015). Yang et al. (2005) reported similar results for the monthly data and corrections across the northern regions. However, the magnitude of P_{max} under-measured varies by precipitation phase, their patterns are very different across the northern regions. The under-measured of P_{max} is small for rain and mixed precipitation (less than 5 mm), and high for snowfall extremes, over 15 mm along the Ural Mountains and the coasts of east Asia, Greenland, in particular northern Eurasia coasts. Hence, in addition to large-scale drivers, regional factors influencing snow precipitation processes, such as wind and temperature, distance from ocean, coastal and mountain ranges, are essential to the variation in P_{max} distribution and bias correction. Apart from the distribution and magnitude of under-measured, the frequency distribution of observed daily snow extremes underestimate significantly the higher risk events over the high latitudes. In light of these findings, there is an urgent need to review and update precipitation datasets and the knowledge of climate regimes and extremes over the broader northern regions.

Automatic gauges with high temporal resolution have been used widely in many countries in recent years.

Bias corrections of hourly precipitation measurements from Geonor-gauges have been applied by Pan et al. (2016) at several sites across western Canada. The World Meteorological Organization Solid Precipitation Intercomparison Experiment (WMO-SPICE) project has developed new methods for auto-gauge bias corrections (Kochendorfer et al., 2017). It is important to point out that the consistency of daily/hourly bias corrections between manual gauges and auto-gauges is major challenge. Hence, this study chooses the period of 1973-2004 using rather consistent daily precipitation data collected by the national manual gauges. Merging the recent data from auto-gauges with the old measurements from manual gauges is necessary to derive reliable and longer term precipitation information. Our effort is on-going to apply the new methods over large regions, including the arctic domain.

Acknowledgements

This study was jointly sponsored by the National Natural Science Foundation of China (NSFC) Grant: 41771262, and the Applied Basic Research of Qinghai Science and Technology Department (Grant: 2019-ZJ-7036).

References

Adam, J., Lettenmaier, D.P., 2003. Adjustment of global gridded precipitation for systematic bias. J. Geophys. Res. 108(D9), 4257. https://doi.org/10.1029/2002JD002499.

Behrangi, A., Gardner, A., Reager, J. T., Fisher, J.B., Yang, D., Huffman, G.J., Adler, R.F., 2018. Using GRACE to estimate snowfall accumulation and assess gauge undercatch corrections in high latitudes. J. Clim. https://doi.org/10.1175/jcli-d-18-0163.1.

Behrangi, A., Christensen, M., Richardson, M., Lebsock, M., Stephens, G., Huffman, G.J., Bolvin, D., Adler, R.F., Gardner, A., Lambrigtsen, B., Fetzer, E., 2016. Status of high-latitude precipitation estimates from observations and reanalyses. J. Geophys. Res. Atmos. https://doi.org/10.1002/2015JD024546.

Brandsma, T., 2014. Comparison of automatic and manual precipitation networks in the Netherlands. De Bilt|Technical Report TR-347.

Changnon, D.A., 2018. Spatial and temporal analysis of 30-day heavy snowfall amounts in the eastern United States 1900–2016. J. Appl. Meteor. Climatol. 57, 319–331.

Coles, S., 2001. An introduction to statistical modeling of extreme values. London: Springer.

Ding, Y.H., Chan, J.C.L., 2005. The East Asian summer monsoon: an overview. Meteorol. Atmos. Phys. 89, 117-142.

Ding, Y., Yang, D., Ye, B., Wang, N., 2007. Effects of bias correction on precipitation trend over China. J. Geophys. Res. 112(D13), D13116. https://doi.org/10.1029/2006JD007938.

Fuchs, T., Rapp, J., Rubel, F., Rudolf, B., 2001. Correction of synoptic precipitation observations due to systematic measuring errors with special regard to precipitation phases. Phys. Chem. Earth B29, 689–693.

289 Gimeno, L., Drumond, A., Nieto, R., Trigo, R.M., Stohl, A., 2010. On the origin of continental precipitation.
290 Geophys. Res. Lett. 37, L13804. https://doi.org/10.1029/2010GL043712.
291 Goodison, B.E., Louie, P.Y.T., Yang, D., 1998. WMO solid precipitation measurement intercomparison.
292 WMO/TD 872 World Meteorol. Org. Geneva 212 pp.
293 Goodison, B.E., Klemm, S., Sevruk, B., 1988. WMO solid precipitation measurement intercomparison Proc.
294 WMO Technical Conference on Instruments and Methods of Observation (TECO-1988) Leipzig GDR
295 16-20 May 1988. WMO/TD No. 222, 255-262.
296 Hanson, L.S., Vogel, R., 2008. The probability distribution of daily rainfall in the United States In World
297 Environmental and Water Resources Congress 2008: Ahupua'A (pp. 1-10).
298 Hartmann, D.L., 2015. Global physical climatology: Second Edition.
299 Jenkinson, A.F., 1955. The frequency distribution of the annual maximum (or minimum) values of
300 meteorological elements. Q. J. Roy. Meteor. Soc. 81,158-171.
301 Jennings, K.S., Winchell, T.S., Livneh, B., Molotch, N.P., 2018. Spatial variation of the rain–snow
302 temperature threshold across the Northern Hemisphere. Nat. Commun. 1148(9),
303 https://doi.org/10.1038/s41467-018-03629-7.
304 Kunkel, K.E., Palecki, M.A., Hubbard, K.G., Robinson, D.A., Redmond, K.T., Easterling, D.R., 2007. Trend
305 identification in twentieth-century U.S. snowfall: The challenges. J. Atmos. Oceanic Technol. 24, 64–73.
306 Kochendorfer, J., Rasmussen, R., Wolff, M., Baker, B., Hall, M. E., Meyers, T., Landolt, S., Jachcik, A.,
307 Isaksen, K., Brækkan, R., Leeper, R., 2017. The quantification and correction of wind induced
308 precipitation measurement errors. Hydrol. Earth Syst. Sci. 21, 1973–1989.

309 Legates, D.R., Willmott, C.J., 1990. Mean seasonal and spatial variability in gauge-corrected global
310 precipitation. Int. J. Climatol. 10, 111–127.

311 Li, N., Li, Y., Yao, N., 2018. Bias correction of the observed daily precipitation and redivision of climatic
312 zones in China. Int. J. Climatol. 38, 3369–3387.

313 López-Moreno, J.I., Vicente-Serrano, S.M., 2011. Effects of climate change on the intensity and frequency
314 of heavy snowfall events in the Pyrenees. Clim. Change 105(3–4), 489–508.

315 O'Gorman, P.A., 2015. Precipitation extremes under climate change. Curr. Clim. Change. Rep. 1, 49–59.

316 Pan, X., Yang, D., Li, Y., Barr, A., Helgason, W., Hayashi, M., Marsh, P., Pomeroy, J., Janowicz, R.J., 2016.
317 Bias corrections of precipitation measurements across experimental sites in different ecoclimatic regions
318 of western Canada. The Cryosphere 10, 2347–2360.

319 Prein, A.F., Gobiet, A., 2016. Impacts of uncertainties in European gridded precipitation observations on
320 regional climate analysis. Int. J. Climatol. 37(1), 305-327.

321 Rajagopal, S., Harpold, A., 2016. Testing and improving temperature thresholds for snow and rain prediction
322 in the western United States. J. Am. Water Res. Assoc. 52, 1142-1154.

323 Scaff, L., Yang, D., Li, Y., Mekis, E., 2015. Inconsistency in precipitation measurements across the Alaska–
324 Yukon border. The Cryosphere 9, 2417-2428.

325 Shabbar, A., Bonsal, B., Khandekar, M., 1997. Canadian precipitation patterns associated with the southern
326 oscillation. J. Climate 10, 3016–3027.

327 Sugiura, K., Ohata, T., Yang, D., 2006. Catch characteristics of precipitation in high-latitude regions with
328 high winds. J. Hydrometeorol. 7, 984–994.

329 Talchabhadel, R., Ramchandra, K., Binod, P., 2017. Intercomparison of precipitation measured between
330 automatic and manual precipitation gauge in Nepal. Measurement 106, 264-273.

331 Tian, X., Dai, A., Yang, D., Xie, Z., 2007. Effects of precipitation-bias corrections on surface hydrology
332 over northern latitudes. J. Geophys. Res. 112, D14101. https://doi.org/10.1029/2007JD008420.

333 Von Mises, R., 1954. La distribution de la plus grande de n valeurs Dans Selected papers American
334 Mathematical Society Providence R.I. II: 271–294.

335 Walsh, J.E., Kattsov, V., Portis, D., Meleshko, V., 1998. Arctic precipitation and evaporation: Model results
336 and observational estimates. J. Clim. 11, 72– 87.

337 Wilson, P.S., Toumi, R., 2005. A fundamental probability distribution for heavy rainfall. Geophys. Res. Lett.
338 32, L14812. https://doi.org/10.1029/2005GL022465.

339 Yang, D., 1999. An improved precipitation climatology for the Arctic Ocean. Geophys. Res. Lett. 26, 1625–
340 1628.

341 Yang, D., Elomaa, E., Tuominen, A., Aaltonen, A., Goodison, B., Gunther, T., Golubev, V., Sevruk, B.,
342 Madsen, H., Milkovic, J., 1999a. Wind-induced precipitation undercatch of the Hellmann gauges. Nordic
343 Hydrology 30, 57–80.

344 Yang, D., Goodison, B.E., Benson, C.S., Ishida, S., 1998a. Adjustment of daily precipitation at 10 climate
345 stations in Alaska: Application of WMO Intercomparison results. Water Resour. Res. 34, 241–256.

346 Yang, D., Goodison, B.E., Metcalfe, J.R., 1998b. Accuracy of NWS 8" standard nonrecording precipitation
347 gage: results and application of WMO intercomparison. J. Atmospheric Ocean. Technol. 15, 54–68.

Yang, D., Goodison, B.E., Metcalfe, J.R., Golubev, V.S., Elomaa, E., Gunther, T., Bates, R., Pangburn, T., Hanson, C.L., Emerson, D., 1995. Accuracy of Tretyakov precipitation gauge: Result of WMO intercomparison. Hydrol. Process. 9(8), 877–895.

Yang, D., Goodison, B.E., Metcalfe, J.R., Louie, P.Y.T., Elomaa, E., Hanson, C.L., Golubev, V., Gunther, T., Milkovic, J., Lapin, M., 2001. Compatibility evaluation of national precipitation gauge measurements. J. Geophys. Res. Atmos. 16, 1481–1491.

Yang, D., Goodison, B.E., Metcalfe, J.R., Louie, P.Y., Leavesley, G.H., Emerson, D.G., Hanson, C.L., Golubev, V.S., Esko, E., Gunther, T., Pangburn, T., Kang, E., Milkovic, J. 1999b. Quantification of precipitation measurement discontinuity induced by wind shields on national gauges. Water Resour. Res. 35, 491–508.

Yang, D., Ishida, S., Goodison, B. E., Gunther, T., 1999c. Bias correction of precipitation data for Greenland. J. Geophys. Res. Atmos. 105, 6171–6182.

Yang, D., Kane, D.L., Hinzman, L.D., Goodison, B.E., Metcalfe, J.R., Louie, P.Y.T., Leavesley, G.H., Emerson, D.G., Hanson, C.L., 2000. An evaluation of the Wyoming gauge system for snowfall measurement. Water Resour. Res. 36, 2665–2677.

Yang, D., Kane, D., Zhang, Z., Legates, D., Goodison, B., 2005. Bias corrections of long-term (1973–2004) daily precipitation data over the northern regions. Geophys. Res. Lett. 32, L19501. https://doi.org/10.1029/2005GL024057.

Yang, D., Ohata, T., 2001. A bias-corrected Siberian regional precipitation climatology. J. Hydrometeorol. 2, 122–139.

368 Ye, B., Yang, D., Ding, Y., Han, T., Koike, T., 2004. A bias-corrected precipitation climatology for China.
369 J. Hydrometeorol. 5, 1147–1160.

370 Ye, B., Yang, D., Ma, L., 2012. Effect of precipitation bias correction on water budget calculation in Upper
371 Yellow River China. Environ. Res. Lett. 7, 025201.

372 Zhang, Y., Ohata, T., Yang, D., Davaa, G., 2004. Bias correction of daily precipitation measurements for
373 Mongolia. Hydrol. Process. 18, 2991–3005.